microprobe x-ray analyzer, while David Fisher and John Bartlett did the atomic absorption analysis. The identification of the anodic films by x-ray and electron diffraction was the work of William Dorfeld and Louis Osika.

Manuscript submitted April 24, 1969; revised manuscript received Aug. 8, 1969. This was Paper 369 presented at the Montreal Meeting, Oct. 6-11, 1968.

Any discussion of this paper will appear in a Discussion Section to be published in the June 1970 JOURNAL.

REFERENCES

1. R. W. Powers, *Electrochem. Technol.*, 5, 429 (1967).
2. R. W. Powers, *ibid.*, 2, 163 (1964).
3. R. W. Powers and M. W. Breiter, *This Journal*, **116**, 719 (1969).
4. H. G. Dietrich and J. Johnston, *J. Am. Chem. Soc.*, **49**, 1419 (1927).
5. Z. Ia. Nikitina, *J. Appl. Chem. USSR*, **31**, 209 (1958).
6. K. Huber, *Helv. Chim. Acta*, **26**, 1037 (1943).
7. K. Huber, *ibid.*, **26**, 1253 (1943).
8. K. Huber, *ibid.*, **27**, 1443 (1944).
9. K. Huber, *This Journal*, **100**, 376 (1953).
10. H. Fry and M. Whitaker, *ibid.*, **106**, 606 (1959).
11. H. Kaesche, *Electrochim. Acta*, **9**, 383 (1964).
12. I. Sanghi and M. Fleischmann, *ibid.*, **1**, 161 (1959).
13. J. Oxley, Leesona Moos Lab. First Quarterly Rpt. to NASA, June-Sept. 1964, Contract No. NAS 5-3908.

The Kinetics of Dissolution of II-VI Semiconductor Compounds in Nonoxidizing Acids

L. D. Locker*,[1] and P. L. deBruyn

Department of Metallurgy and Materials Science, Massachusetts Institute of Technology, Cambridge, Massachusetts

ABSTRACT

The dissolution of ZnS, CdS, ZnSe, and $Zn_{0.85}Cd_{0.15}S$ in acid solutions has been studied under conditions where the group VI anions yield only H_2S or H_2Se. The activation energies depend on the particular compound, the acid, and the solvent. However, for ZnS the activation energy is independent of purity and crystal structure. For dissolution of high-purity compounds in aqueous H_2SO_4, the activation energies (kcal/mole) are: ZnS(9.5), CdS(14.2), ZnSe(11.7). The factors that determine nonoxidative dissolution kinetics are analyzed, and a model is presented. This case is compared to the mechanism of elemental and compound semiconductor dissolution where electron transfer occurs, and there is a relatively large change in the oxidation states between reactants and products.

The atomic processes that occur on the surface of a solid during dissolution depend on the type of bonding in the solid and on the particular species in solution (1-5). For the electrochemical dissolution of semiconductors, these processes have been studied extensively. However, little attention has been given to the mechanism of dissolution of semiconductors in nonoxidizing solutions.

The relationship of structure and bonding to the dissolution mechanism can be illustrated by several cases. For example, the dissolution of alkali halide crystals, such as LiF, is analogous to evaporation in that atoms are removed by dissociation from kink sites on the surface (1, 2). If the initial rate of dissolution in pure solvents is expressed by the equation

$$R_o = \nu \exp(-E/RT) \qquad [1]$$

then for the alkali halides ν is a frequency factor that depends on the surface area and the distribution of active sites, and the activation energy E is the energy for dissociation of surface atoms. In the anodic dissolution of semiconductors, the rate is often controlled by the transport of holes from the bulk of the semiconductor to the surface. The pre-exponential term in Eq. [1] will then be a function of the bulk charge carrier concentration, the charge of the carriers, the diffusion coefficient, and the characteristic diffusion length in the solid. The activation energy will be influenced by space charge effects in the solid as well as by the bonding and structure of the particular semiconductor. All factors that have an influence on the charge carrier concentration will affect the rate of dissolution (*e.g.*, illumination, n- or p-type impurities, temperature, injection by a p-n junction, and reduction of oxidants such as ferricyanide ions on the surface).

For heavily doped n-type germanium, Gereth and Cowher (3) have reported that the rate of anodic dissolution is controlled by the supply of hydroxyl ions from the electrolyte, rather than by charge carriers in the solid. Therefore, the activation energy may depend on space charge layers in the solution rather than in the semiconductor. The pre-exponential in Eq. [1] will then be proportional to the hydroxyl ion concentration. In addition, for the spontaneous dissolution of germanium in oxygen-saturated media, Harvey and Gatos (4) found that the rate is independent of carrier concentration or illumination. In oxidative dissolution such as this, when diffusion is not rate limiting, it is bond breaking in an oxide surface complex that determines the activation energy. ν is then related to the frequency of thermal vibrations in the solid.

To distinguish between oxidative and nonoxidative dissolution, Simkovich and Wagner (5) showed for PbS and ZnO that doping of the solid and deviations from stoichiometry do not have a significant effect on the rate of dissolution in nonoxidizing acids, such as aqueous HCl. However, Ag_2S as an acceptor and Bi_2S_3 as a donor in PbS, or Li_2O as an acceptor and Al_2O_3 as a donor in ZnO do significantly affect the rate of dissolution in concentrated nitric acid. The oxidative dissolution can be characterized by the formation of elemental sulfur as a reaction product in the case of PbS.

Based on the above results, it can be concluded that in nonoxidative dissolution the rate constant and the activation energy in Eq. [1] are related to processes that occur at the solid-liquid interface. To investigate

* Electrochemical Society Active Member.
[1] Present address: Bell Telephone Laboratories, Murray Hill, New Jersey.

these processes in acid solutions, the dissolution of the II-VI compounds ZnS, ZnSe, CdS, and solid solution $Zn_xCd_{1-x}S$ has been studied as a function of both the structure and composition of the solids, and the properties of the solution. The over-all chemical reaction describing the dissolution process is

$$A_{II}B_{VI}(s) + 2H^+ = A_{II}^{++} + H_2B_{VI}(g) \qquad [2]$$

with A_{II} representing the group IIB cation and B_{VI} the group VI anion. The II-VI compounds are particularly suitable for studying nonoxidative dissolution kinetics for several reasons:

1. It has already been shown that in well-agitated systems the rate is controlled by a heterogeneous surface reaction rather than by transport in the solution (6).
2. The reaction products do not form passive films that could inhibit the dissolution process.
3. The compounds can be prepared in allotropic crystalline modifications, and have a complete range of solid solubility.

Experimental

Materials.—All of the polycrystalline II-VI compounds were prepared by precipitation from a soluble salt of the group IIB cation. To produce a crystalline solid, the precipitate was dried, and annealed in H_2B gas or in an inert atmosphere. The method of preparation, impurity content, B.E.T. surface area, and crystal structure of each material are summarized in Table I. The composition of the crystallized solid solution was determined by comparing the measured lattice parameters to those reported by Ballentyne (7). In addition, chemical analyses for both zinc and cadmium were done after completely dissolving the solid in cold concentrated hydrochloric acid or in nitric acid. These two analytical methods gave results that were within 4%. The composition determined by x-ray analysis is reported in Table I. Reagent-grade chemicals and high-conductivity water (6.0×10^{-7} ohm^{-1} cm^{-1}) were used to prepare the acid solutions.

Apparatus and procedure.—Except for dissolution of ZnSe, rate measurements were made at constant pressure by continuously increasing the volume of the system as vapor was evolved. The pressure regulating system was similar to the one described by Cremer (8), although modifications were needed to keep the pressure constant to within 0.1 mm Hg while automatically recording the volume (9). The evolution of as little as 3×10^{-7} moles of vapor could be detected. This sensitivity is required in order to study the dissolution of the sparingly soluble II-VI compounds.

A 200-ml baffled Pyrex reactor flask, shown in Fig. 1, was immersed in a constant-temperature bath controlled to within 0.1°C. All experiments were carried out at a stirring speed of 1200 rpm. A 3g solid sample (± 0.1 mg) was held in a thin-walled Pyrex crucible before the start of each reaction so that it did not contact the acid in the flask. Fifty milliliters of acid

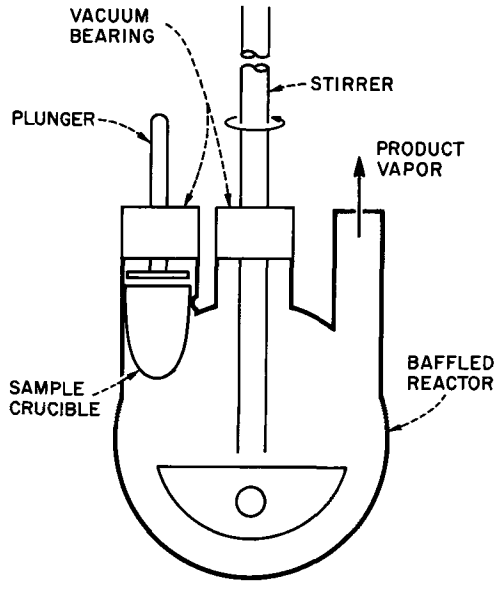

Fig. 1. Stirred reactor and sample crucible

solution were degassed by lowering the pressure until the solution boiled. The solution was then saturated by flushing the system with H_2S vapor. With the stirrer on, the reaction started instantaneously when the plunger pushed the sample crucible into the acid solution.

Dissolution experiments performed at constant pressure and temperature have definite advantages compared to experiments at constant volume. All of the vapor produced in the reaction goes into the gas phase since the solution is already saturated at a fixed constant pressure. Also, the evaluation of the constants in an empirical rate equation is easier when both temperature and pressure are constant during an experiment. In principle, the constant-pressure apparatus could have been used for the ZnSe experiments, but the large quantities of H_2Se needed to flush the system made this impractical. Although the ZnSe experiments were done at constant volume, the same reactor was used for all experiments and the sample was introduced in the same way as described above.

The concentration of acid, zinc ions, and cadmium ions was determined after equilibrium was reached in each experiment. For both zinc and cadmium, volumetric analysis was used, with ethylenediaminetetracetic acid as a complexing agent. In addition, when the cadmium ion concentration was too small to be determined by volumetric methods, analyses were done with a Jarrel-Ash flame photometer.

Results

Typical examples of the kinetic data collected in this investigation are displayed in Fig. 2 and 3. The dependence of the dissolution rate of high-purity ZnS

Table I. Preparation and properties of materials

Material	Method of preparation	Impurity content (spectroscopic analysis)	Crystal structure (observed values)	Surface area (m^2/g)
ZnS	$Zn(NO_3)_2 + H_2S$	10 ppm: Pb 3 ppm, Cu 0.2 ppm, Ni 0.3 ppm, Fe 1 ppm	Cubic $a_o = 5.38$Å	28.8
ZnS	$ZnSO_4 + H_2S$	2%: Cd 1%, Fe 0.1%	75% cubic-25% hex. (approximate)	5.5
CdS	$Cd(NO_3)_2 + H_2S$	10 ppm	Hexagonal $a_o = 4.12$Å $c_o = 6.94$Å	0.94
ZnSe	$Zn(Cl)_2 + (NH_4)_2Se$	10 ppm	Cubic $a_o = 5.60$Å	0.63
$Zn_xCd_{1-x}S$ $X = 0.85$	$Zn(C_2H_3O_2)_2 + Cd(C_2H_3O_2)_2 + H_2S$	No analysis	Hexagonal $a_o = 3.86$Å $c_o = 6.30$Å	1.2

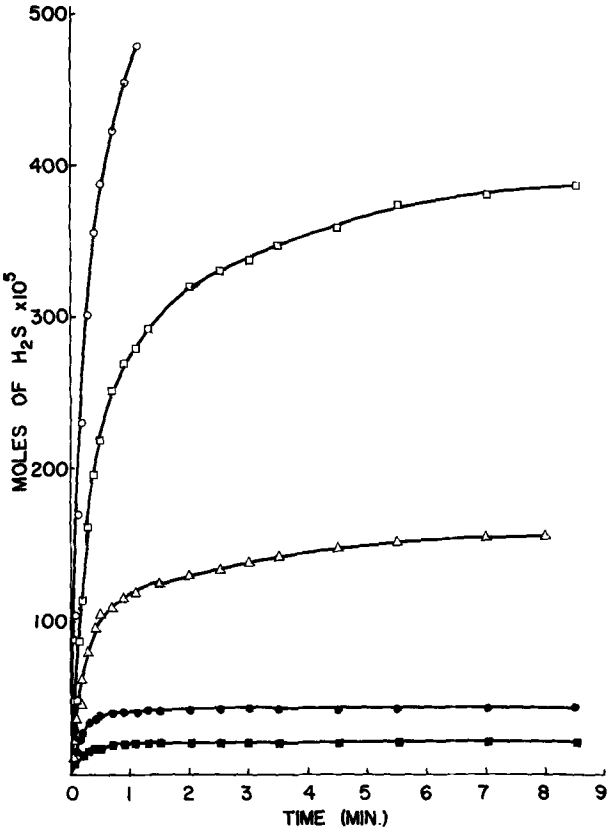

Fig. 2. Effect of sulfuric acid concentration on the dissolution of high-purity ZnS: ■ 0.5M; ● 1.0M; △ 2.0M; □ 3.0M; ○ 4.0M; T = 25°C; p_{H_2S} = 0.88 atm.

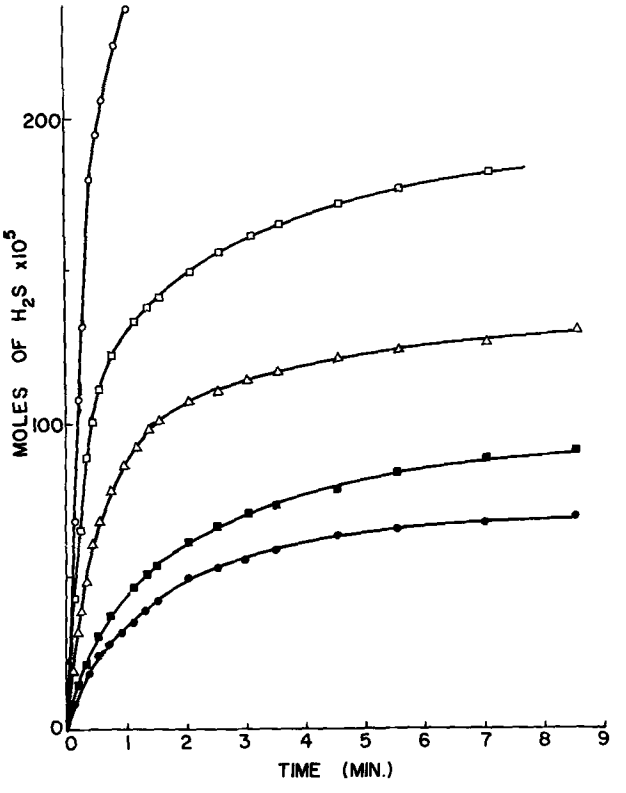

Fig. 3. Effect of temperature on the dissolution of high-purity ZnS in aqueous H_2SO_4: ● T = 0.2°C p_{H_2S} = 0.26 atm; ■ T = 10.0°C p_{H_2S} = 0.15 atm; △ T = 25.0°C p_{H_2S} = 0.27 atm; □ T = 40.0°C p_{H_2S} = 0.25 atm; ○ T = 59.0°C p_{H_2S} = 0.40 atm; [H_2SO_4] = 1.0M.

on sulfuric acid concentration at fixed temperature and hydrogen sulfide pressure is illustrated in Fig. 2. Figure 3 shows the variation of the dissolution rate with temperature at constant sulfuric acid concentration (1M). In all the investigations, the dissolution was allowed to proceed to conclusion so that information on the equilibrium state may also be obtained. This information is needed in order to determine the kinetic parameters of the reverse (precipitation) reaction. Although the general shape of the dissolution curves does not change with the composition of the leaching solution (aqueous sulfuric acid, alcoholic sulfuric acid, or aqueous hydrochloric acid), the dissolution rate in aqueous sulfuric acid is found to depend more strongly on temperature than in the other two solutions.

Our experiments confirmed the finding of Romankiw and deBruyn (6) that the dissolution process is independent of the rate of agitation of the reacting mixture beyond a critical stirring speed of 750 rpm. This experimental observation suggests that the net dissolution rate is not diffusion controlled. If we now assume that the dissolution process is controlled by a chemical reaction at the solid-liquid interface, then the rate of dissolution R (moles/m^2 sec) may be expressed as follows:

$$R = \frac{1}{A}(dn_{H_2B}dt) = k_1[H_2SO_4]^{\alpha} - k_{-1}[A_{II}SO_4]^{\beta}p^{\gamma}{}_{H_2B} \quad [3]$$

In writing Eq. [3], we assume the leaching agent to be sulfuric acid. The various symbols introduced in this expression are identified in the Nomenclature at the end of this paper. It is important to note that the formal rate constants k_1 and k_{-1} for the forward and reverse reactions, respectively, include the activity coefficients of the reacting species. The symbol A without subscript refers to the surface area (m^2) of the solid/liquid interface. The square brackets, [], imply molar concentrations of the reactants; the quantity [H_2SO_4] refers to the stoichiometric sulfuric acid concentration and not to the molar concentration of the undissociated species.

Spectrophotometric studies (10) of the composition of aqueous sulfuric acid solutions show that, except in extremely dilute solutions, the $SO_4^=$ ion is not a major constituent and that the concentration of undissociated H_2SO_4 is negligibly small in solutions of molarity less than 14M. At moderate concentrations, it is the HSO_4^- ion which predominates and the properties of such solutions are essentially that of a 1:1 electrolyte consisting of H^+ and HSO_4^- ions. An analysis of all pertinent thermodynamic data on this system in the temperature range 0°-50°C (11) shows that the H^+ ion concentration is proportional to the stoichiometric acid concentration in the concentration range 0.1-6M which includes the experimental concentrations (0.5-5M) used in this investigation. The sulfuric acid concentration term in Eq. [3] may therefore be replaced by the actual concentration of H^+, the proportionality constant relating [H^+] to [H_2SO_4] being approximately 0.8.

To determine the order of the forward reaction, that is, the magnitude of the constant α, we focus attention on the initial stage of the dissolution reaction. Equation [3] may now be transformed to read

$$R_o = k_f A_o[H_2SO_4]_o^{\alpha} \exp(-E_f/RT) \quad [4]$$

where R_o is the initial dissolution rate in moles/sec and is given by the initial slope of the experimental curves in Fig. 2. A check on the measured value of R_o was obtained by a numerical curve fitting technique (9). By plotting values of R_o against initial acid concentration ([H_2SO_4]$_o$), it was clearly established that α equals unity regardless of the composition of the solid phase and of the liquid phase. This first-order dependence of the dissolution rate on acid concentration was previously observed by Romankiw and deBruyn (6) for ZnS in aqueous sulfuric acid solutions. These

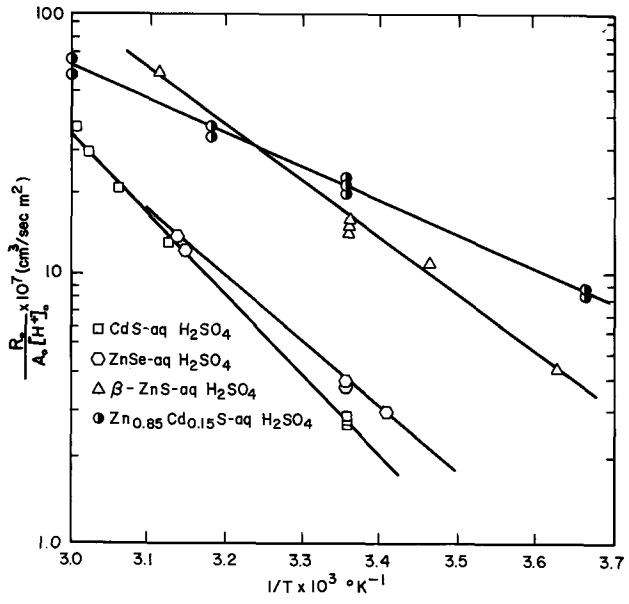

Fig. 4. Arrhenius plot for calculation of the activation energies for dissolution of II-VI compounds in aqueous H_2SO_4.

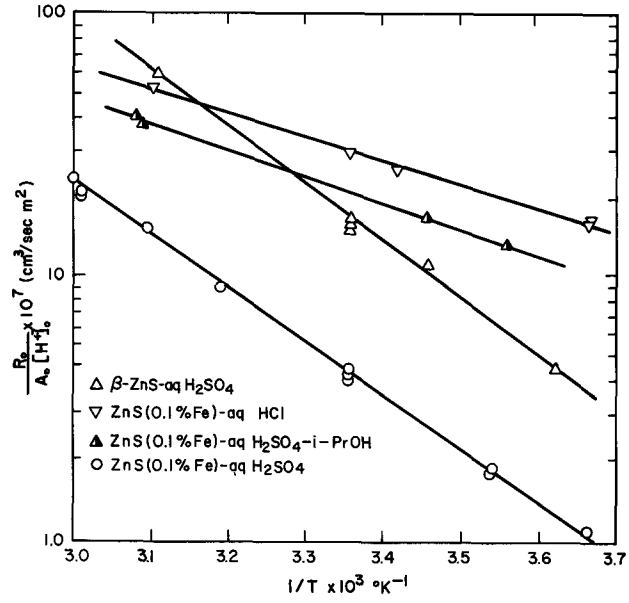

Fig. 5. Arrhenius plot for calculation of the activation energy for dissolution of ZnS in different solutions.

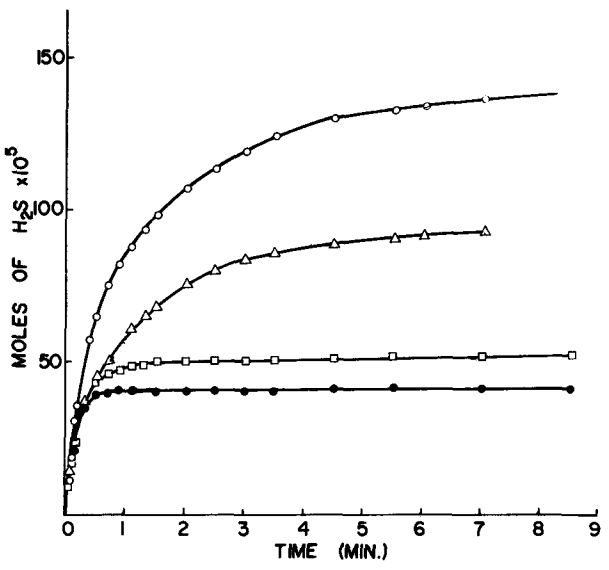

Fig. 6. Effect of H_2S pressure on the dissolution of high-purity ZnS in aqueous H_2SO_4: ● p_{H_2S} = 0.27 atm; △ p_{H_2S} = 0.32 atm; □ p_{H_2S} = 0.82 atm; ○ p_{H_2S} = 1.01 atm; T = 25°C; $[H_2SO_4]$ = 1.0M.

authors used an identical analytical procedure for evaluating α.

The activation energy E_f for the forward (dissolution) reaction was then determined by preparing plots of log $(R_o/A_o[H_2SO_4]_o)$ = log k_1 against $1/T$ as shown in Fig. 4 and 5. The magnitude of k_f, a reaction rate constant which is independent of temperature, may then be calculated.

At constant pressure of H_2B, it follows directly from Eq. [3] that for equilibrium conditions

$$d \log [A_{II}^{++}]_e / d \log [H^+]_e = \beta \qquad [5]$$

where the subscript e denotes that the equilibrium concentrations of the reacting species are to be used. Equation [5] shows how the constant β for the reverse (precipitation) reaction may be evaluated from experimental data such as found in Fig. 2. It also follows from Eq. [4] that, if the initial concentration of the acid is fixed in a series of experiments in which the pressure of the H_2B gas is allowed to vary, then at equilibrium, for $\alpha = 1$,

$$\log \left\{ \frac{[H_2SO_4]_o - [A_{II}SO_4]_e}{[A_{II}SO_4]_e{}^{\beta}} \right\} = \gamma \log p_{H_2B} + \log \frac{k_{-1}}{k_1} \qquad [6]$$

and therefore

$$\frac{d \log \{([H_2SO_4]_o - [A_{II}SO_4]_e)/[A_{II}SO_4]_e{}^{\beta}\}}{d \log p_{H_2B}} = \gamma \qquad [7]$$

Once β is known, the constant γ may be evaluated from the information contained in experimental rate curves such as those plotted in Fig. 6. From the appropriate plots suggested by Eq. [5] and [7], it has been established that the rate of the reverse reaction varies with the *square root* of both the concentration of the A_{II}^{++} ion in solution and the H_2B pressure. The activation

Table II. Activation energies and rate constants

Material	Solution composition	E_f (kcal/mole)	k_f (liters/sec m²)	E_r (kcal/mole)	k_r (moles liters/atm)$^{1/2}$ / sec m²
ZnS (0.1% Fe)	aq. H_2SO_4	9.9 ± 1.0*	2.7 ± 0.4 × 10^1	6.7 ± 1.0	1.9 ± 0.5 × 10^0
	aq. 20%-i-PrOH≠ 80% H_2SO_4	5.0	8.9 × 10^{-3}	1.6	5.3 × 10^{-4}
	aq. HCl	4.5	5.4 × 10^{-3}	—	—
β-ZnS	aq. H_2SO_4	9.5	3.8 × 10^0	5.8	7.5 × 10^{-2}
CdS	aq. H_2SO_4	14.2	6.8 × 10^3	6.7	1.7 × 10^1
ZnSe	aq. H_2SO_4	11.7	1.0 × 10^2	6.8	4.8 × 10^1
$Zn_{0.85}Cd_{0.15}S$	aq. H_2SO_4	5.7	2.9 × 10^{-2}	5.3	3.4 × 10^1

* Precision noted for the first value applies to others in same column.
≠ i-PrOH represents isopropanol.

energy (E_r) of the reverse (precipitation) reaction was then determined by solving Eq. [6] for k_{-1} at different temperatures and then plotting log k_{-1} against $1/T$.

All the pertinent kinetic parameters obtained by the above analysis of the experimental data are collected in Table II. It should be mentioned that in performing this analysis no correction has been made for the dependence of the activity coefficient of the reacting species on temperature. However, the stoichiometric activity coefficients for sulfuric acid and also hydrochloric acid in the concentration range 0.5*M* (Molal) to 5*M* are relatively insensitive to changes in temperature (12). The magnitudes of the activation energies E_f and E_r will therefore not be altered significantly if such corrections are made.

It is interesting to note for Table II that the values of E_r for ZnS, ZnSe, and CdS agree to within ±1 kcal/mole. During the asymptotic approach to equilibrium shown in Fig. 2, 3, and 6, the solid must form simultaneously with the dissolution. The reverse reaction involves either precipitation of new particles or growth on the already existing solid. In either case, the data suggest that the process of solid formation is not simply the reverse of the dissolution process. No attempt has been made to study the reverse reaction in detail, since the initial rate data used to calculate k_f and E_f are not affected by these complexities.

In Table II it can be seen that the activation energy E_f for dissolution in aqueous H_2SO_4 is different for each of the high-purity II-VI compounds. However, for the high-purity β-ZnS, the activation energy is almost the same as for the material containing 0.1% Fe. The latter solid also showed some wurtzite lines in its x-ray diffraction pattern which did not appear in the high-purity β-ZnS. These results indicate that the activation energy is not sensitive to impurity content or crystal structure, but the over-all rate of dissolution does depend on these factors due to changes in the number of reactive surface sites.

The dependence of the dissolution rate on the properties of the solution are also shown in Table II. For the same solid ZnS(0.1% Fe) in different solutions, there is a large change in the activation energy. Therefore, changing the solution, and with it the properties of the solid-liquid interface, influences the activation energy for the rate-controlling step.

The relatively low activation energy for dissolution of the solid solution $Zn_{0.85}Cd_{0.15}S$ may be related to other observations made on this material. For example, even after heat treatment, the x-ray diffraction peaks of the crystallized solid were not nearly as sharp as for the pure ZnS or CdS. It was found that the Zn/Cd ratio in the solution was several times higher than the ratio in the starting material. Therefore it is possible that the method of preparation sufficiently influences the surface properties of the solid to affect the activation energy for dissolution.

The results show that the rate of nonoxidative dissolution depends on both the properties of the solid and the solution. These data bear out the introductory remarks that any proposed mechanism of nonoxidative dissolution of semiconductors must account for the influence of processes at the solid-liquid interface.

Discussion

Figure 7 shows the steps that occur during dissolution of the II-VI compounds in nonoxidizing acids. Since agitation has no influence on the rate of dissolution of the II-VI compounds in aqueous H_2SO_4, and the activation energies are higher than the 3-6 kcal/mole expected for transport processes, it is unlikely that diffusion is the rate-controlling step. Furthermore, a quantitative estimate of the rate of diffusion of H^+ can be made using the equation

$$\frac{1}{A}(dn_{H_2B}/dt) = -D([H^+]_o - [H^+]_i)/d \qquad [8]$$

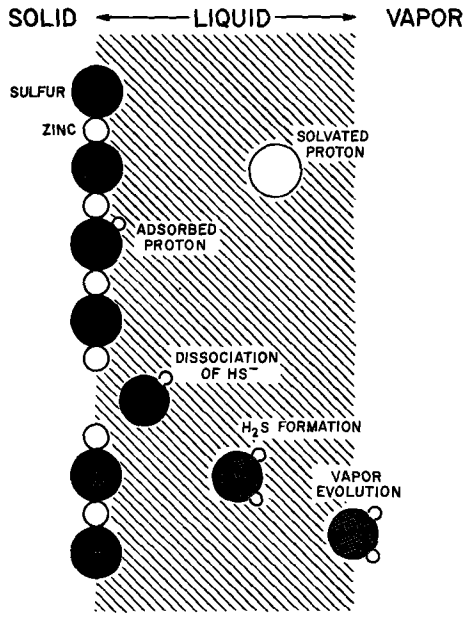

Fig. 7. The mechanism of dissolution of II-IV compounds in nonoxidizing acids.

where $[H^+]_i$ is the concentration of hydrogen ions near the solid surface. Values of $[H^+]_i = 0$, $[H^+]_o = 2$ moles/liter, $d = 10^{-3}$ cm, and $D = 10^{-5}$ cm²/sec, give a rate of 10^{-5} moles/(sec cm²). The chosen values of the effective boundary layer thickness, d, and the diffusivity, D, are likely to be within an order of magnitude for this system. Experimentally, for the II-VI compounds in aqueous H_2SO_4, the initial rates were no larger than 10^{-9} moles/(sec cm²). For the dissolution of ZnS in hydrochloric acid or in alcoholic H_2SO_4, the initial rates were approximately 10^{-5} moles/(sec cm²), so that the exclusion of diffusion control here is not as certain. However, it is the fact that the surface reaction is much slower for dissolution of ZnS in aqueous H_2SO_4 than in the other solutions, rather than the magnitude of the activation energy in the latter case, that is important. This fact is used below as evidence that a slow adsorption step is a plausible mechanism for the dissolution of the II-VI compounds in nonoxidizing aqueous H_2SO_4.

If the over-all rate of the dissolution reaction is controlled by the adsorption of hydrogen ions, or the protonated solvent, onto the surface then

$$R_o = k_f A_o [H^+]_i \exp(-E_A/RT) \qquad [9]$$

E_A is the activation energy for adsorption of the hydrogen ions at the interface. The concentration $[H^+]_i$ is related to the concentration in the bulk solution by the equation

$$[H^+]_i = [H^+]_o \exp(-\psi_\delta/RT) \qquad [10]$$

where ψ_δ is the potential of the ion at the distance of closest approach, before adsorption onto the surface. As hydrogen ions adsorb there is a change in potential equal to $(\psi_o - \psi_\delta)$, where ψ_o is the potential of the solid surface relative to the bulk solution. Also there is an energy change, Φ, when a proton interacts with the surface atoms to form some compound. This free energy change will depend on the activity of the solid surface, but it is independent of the surface charge. As shown in Fig. 7, it is assumed that the hydrogen ions adsorb preferentially on the sulfur sites, and that the surface reaction product dissociates as HS^-. This ion then reacts with a hydrogen ion to form H_2S which is transported away from the solid, and is finally evolved at the liquid-vapor interface. The observation that the H_2S/Zn^{++} mole ratio is greater than 1 is reasonable if adsorption occurs preferentially at the sulfur sites.

In terms of the adsorption theory of dissolution, where no electron transfer is involved in the rate-controlling step, the rate equation becomes

$$R_o = k_f A_o [H^+]_o \exp\left\{-\frac{\mathbf{F}}{RT}[\Phi + (\psi_o - \psi_\delta) + \psi_\delta]\right\} \quad [11]$$

The activation energy for dissolution, with the adsorption step controlling is

$$E_A = \mathbf{F}(\Phi + \psi_o) \quad [12]$$

E_A is made up of a chemical and an electrostatic contribution. The former can be related to the bonding, surface energy, and other solid properties that may effect Φ. The latter term depends on the interaction between the charged solid surface and the ions in solution. Changes in the activity of the surface due to the structure or the composition of the solid will generally be small, and Φ will not be appreciably changed. This is the reason for the small difference between the activation energies for pure β-ZnS and ZnS(0.1% Fe). The model also explains the results of Simkovich and Wagner (5), that impurities in the solid have little effect on the rate of nonoxidative dissolution. The low activation energy for $Zn_{0.85}Cd_{0.15}S$ is probably due to a state of disorder of the surface that is sufficient to affect the chemical potential for proton adsorption.

The maximum difference of about 5 kcal in the activation energies for dissolution of ZnS, ZnSe, and CdS is due primarily to the electrostatic interaction at the solid-liquid interface. This also must account for the changes in the activation energy when the same solid ZnS is dissolved in different solutions. For hydrochloric acid as the solvent, there is also the possibility that specific interactions of chloride ions occur on the surface, and alter both the surface charge and the distribution of active sites. This would lead to changes in both the rate constant and the activation energy. Although the concept of a dielectric constant for the solution near the solid surface has little meaning, the polarizability of the solvent and the potential drop across the Helmholtz layer are essential factors in the mechanism of nonoxidative semiconductor dissolution.

Conclusion

The experimental results, analyzed in terms of an activated adsorption model for the dissolution of II-VI compounds, explain why the rate of dissolution in nonoxidizing solutions is not affected by the electrical properties of the solid. It is the space charge in the solution rather than in the solid that is important.

Even in the case of oxidative semiconductor dissolution, it is known that adsorption affects the kinetics by increasing or decreasing the rate of the controlling step. For example, in the oxidative dissolution of InSb, which exhibits crystallographic polarity in the <111> direction, aliphatic amines preferentially adsorb on the Sb(111) surface and inhibit the rate by interfering with dissociation of the surface complex that controls the rate of dissolution (13). Richards and Crocker (14) found that Ag^+ reveals etch pits on the As(111) surface of GaAs for the same reason. In these two cases, it is the rate constant k_1 in Eq. [1] that is lowered. According to Harvey and Gatos (4), adsorbed halide ions catalyze the reduction of oxygen on the surface of Ge by supplying one electron. Based on the mechanism of dissolution proposed by Harvey and Gatos, this adsorption effects E as well as k_1 in Eq. [1]. Adsorbed ions can also change the rate of anodic dissolution of semiconductors when charge transfer in the solid is the rate-controlling step. The reduction of ferricyanide ($Fe(Cn_6^{-3})$ to ferrocyanide ($Fe(CN_6^{-4})$ on the germanium surface leads to an increase in the anodic dissolution rate. This is explained by Efimov (15) by the supposition that the electron required for the reduction comes from the valence band, creating an additional hole near the germanium surface. The process is analogous to the effect of illumination on the charge transfer controlled anodic dissolution.

In nonoxidative dissolution of the II-VI compounds, it is the adsorption that is the rate-controlling step. The adsorption model may be useful in explaining the results of etching studies in nonoxidizing solutions. According to this model, preferential adsorption occurs on the anion sites so that this face would be expected to dissolve faster than the corresponding cation face when the II-VI compounds are etched in the (111) orientation. Therefore, etch pits should appear on the cation faces. Studies of the adsorption kinetics of ions at the semiconductor-electrolyte interface and a more complete understanding of the changes in solvation that occur in the layer of solution near the solid surface would permit this adsorption theory of semiconductor dissolution to be developed further. These same effects are important in a broader scope of electrochemistry, such as with anodic oxide films and battery electrode behavior, so that the adsorption mechanism of nonoxidative semiconductor dissolution may be of more general importance.

Manuscript submitted March 7, 1969; revised manuscript received Aug. 8, 1969.

Any discussion of this paper will appear in a Discussion Section to be published in the June 1970 JOURNAL.

REFERENCES

1. I. Gallily and S. K. Friedlander, *J. Chem. Phys.*, **42**, 1503 (1965).
2. M. B. Ives, *J. Phys. Chem. Solids*, **24**, 275 (1963).
3. R. Gereth and M. E. Cowher, *This Journal*, **114**, 147C (1967).
4. W. W. Harvey and H. C. Gatos, *ibid.*, **105**, 654 (1958).
5. G. Simkovich and B. Wagner, *ibid.*, **110**, 513 (1963).
6. L. T. Romankiw and P. L. deBruyn, "Unit Operations in Hydrometallurgy," M. Wadsworth, Editor, p. 45, Gordon and Breach (1965).
7. D. W. G. Ballentyne and B. Ray, *Physica*, **27**, 337 (1961).
8. E. Cremer *et al.*, *Radex-Rundschau*, **1953**, 495.
9. L. D. Locker, Ph.D. Thesis, M.I.T. (1965).
10. T. F. Young, *Record Chem. Progr.*, **12**, 81 (1951).
11. L. T. Romankiw, S. M. Thesis, M.I.T. (1962).
12. H. S. Harned and B. B. Owen, "The Physical Chemistry of Electrolytic Solutions," Third Ed., Reinhold Publishing Corp., New York (1958).
13. H. C. Gatos and M. C. Lavine, *J. Phys. Chem. Solids*, **14**, 169 (1960).
14. J. L. Richards and A. J. Crocker, *J. Appl. Phys.*, **31**, 600 (1960).
15. E. A. Efimov, "Electrochemistry of Germanium and Silicon," Sigma Press (1963).

NOMENCLATURE

A	Surface area of solid (m^2)
A_o	Surface area of solid at start of reaction (m^2)
A_{II}	Atom of group IIB (Zn, Cd)
A^{++}, A_{II}^{++}	Ion of A_{II} in solution
$[A^{++}]_e$	Ion concentration at equilibrium (moles/liter
B, B_{VI}	Atom of group VIB (S, Se)
d	Diffusion path length (cm)
D	Diffusivity (cm^2/sec)
E	Activation energy (kcal/mole)
E_A	Activation energy for proton adsorption (kcal/mole)
E_f	Activation energy for dissolution reaction (kcal/mole)
E_r	Activation energy for precipitation reaction (kcal/mole)
$\mathbf{F}$	Faraday constant
$[H_2SO_4]_o$	Acid concentration at start of reaction (moles/liter)
$[H_2SO_4]_e$	Acid concentration at equilibrium (moles/liter)
$[H^+]_i$	Hydrogen ion concentration at solid-liquid interface (moles/liter)
k_1	Formal forward rate constant $\left(\frac{\text{liters}}{m^2\ \text{sec}}\right)$

k_{-1} Formal reverse rate constant $\left[\frac{\text{moles}}{\text{m}^2\,\text{sec}} \cdot \left(\frac{\text{liters}}{\text{moles}}\right)^{1/2} \cdot \left(\frac{1}{\text{atm}}\right)^{1/2}\right]$

k_f Rate constant for dissolution (liters/sec m^2)

k_r Rate constant for precipitation (moles liter/atm)$^{1/2}$/sec m^2

n_{H_2B} Moles of vapor evolved in reaction

p_{H_2B} Pressure of H_2B vapor (atm)

R_o Initial rate of dissolution (moles/sec)

R Over-all reaction rate (moles/m^2 sec)

T Temperature (°K)

ν Frequency factor

ψ_δ Electrostatic potential of proton at solid-liquid interface relative to bulk solution

α, β, γ Constants

ψ_o Electrostatic potential of proton on solid surface relative to bulk solution

Φ Change in chemical potential during proton adsorption

Interpretation and Significance of Heats of Activation for Electrochemical Reactions Exhibiting Anomalous Tafel Slopes

B. E. Conway and D. J. MacKinnon

Department of Chemistry, University of Ottawa, Ottawa, Ontario, Canada

ABSTRACT

Heats of activation for electrochemical reactions studied over a wide range of temperatures are considered in relation to the temperature dependence of the Tafel slope factor b. Experimentally, b is found to have anomalous temperature dependence, *i.e.*, other than the classical form $RT/\alpha\mathbf{F}$, for hydrogen evolution at Hg, Cd, Pb, Ni, and Pt and the consequences of this behavior in calculation of heats of activation are evaluated. Curvature of the electrochemical Arrhenius plots is shown to arise for certain of the cases treated and is discussed in relation to the problem of detection of proton tunneling at low temperatures. Other difficulties associated with temperature dependence of coverage by atomic H and temperature-dependent structure changes in the solvent are considered.

Heats of activation in electrode processes, unlike those for gas phase and in certain cases solution reactions, cannot be easily related to the mechanism of the reaction. This arises because only an apparent energy of activation (1) is measured by such experimental derivatives as $d \ln i_o/d(1/T)$ (involving the exchange current density i_o), $(d\eta/dT)_i$, $(d\eta/d\ 1/T)_i$ or $(d\eta/d \ln T)_i$, where η is the overpotential at a current density i related to i_o by the familiar equation $i = i_o \exp \eta/b$, where b is the Tafel slope. However, in a number of situations, variations of heats of activation for a given reaction, *e.g.*, over a series of metals, or on account of isotopic substitution, or with temperature, can be useful as a basis for evaluation of such factors as chemisorption in relation to the electronic character of the metal (2) or the role of quantum-mechanical tunnel effects in proton transfer (3) through the estimation of frequency factor ratios.

Normally the apparent heat of activation $\Delta H^{o\neq}_R$ at the reversible potential differs from the "true," kinetically significant quantity $\Delta W^{o\neq}$ (for zero metal-solution p.d.) according to the relation (1)

$$\Delta H^{o\neq}_R = \Delta W^{o\neq} - \beta \Delta H^o \qquad [1]$$

where ΔH^o is the enthalpy change in the single (half-cell) reaction

$$H^+_{aq} + e_M \rightleftharpoons \tfrac{1}{2} H_2 \qquad [2]$$

and β is a symmetry factor. It is well known that ΔH^o, for obvious reasons, is not a thermodynamically measurable quantity, although it may be estimated with varying degrees of uncertainty depending on the value assigned to the surface potential and the basis for assignment of individual ionic free energies of hydration (4).

Usually the apparent heat of activation is evaluated at zero overpotential from the derivative $(\partial \ln i_o/\partial\ 1/T)_{\eta=0}$ or from the temperature coefficient of overpotential at a given current density (5). At finite overpotential η, the derivative $(\partial \ln i/\partial\ 1/T)_\eta$ also gives the effective heat of activation at potential η which differs from that deduced for the reversible potential by the energy $\beta\eta\mathbf{F}$. These relations which give $\Delta H^{o\neq}_R$ in terms of $\Delta W^{o\neq}$ and ΔH^o apply when the Tafel slope b of the process is given by $b = RT/\beta\mathbf{F}$ and $\beta \neq f(T)$.

In the present and other (6) recent work, we have investigated the temperature dependence of the Tafel slopes of the hydrogen (h.e.r.) and bromine evolution reactions over a wide range of temperatures (including low temperatures down to −125°C) in order to establish the correct form of the temperature dependence of b. It has been found (6) that b is rarely given by the "defining" relation quoted above and usually b is less temperature dependent than is implied by $b = RT/\beta\mathbf{F}$ with β a constant equal to approximately 0.5. Under some conditions b can be almost independent of temperature (6-9), while for other conditions b may even increase with decreasing temperature. Inspection of early papers in the literature reveals qualitatively similar observations, but the results were usually poorly reproducible and were obtained in insufficiently purified solutions. Also, the variation of b or β with T was not systematically examined.

Generally (6), when $b \neq RT/\beta\mathbf{F}$, the Tafel slope can be represented empirically by

$$b = \frac{RT}{\beta\mathbf{F}} + c \qquad [3]$$

where c is a temperature independent constant and β can be > 0.5. It appears coincidental that $b = 0.116$ at room temperature, *e.g.*, for the h.e.r. at Hg, so that b is apparently $RT/\beta\mathbf{F}$ with $\beta = 0.5$. Over a wider range of temperature, including low temperatures down to −100°C in methanol and ethanol (3, 6), and higher temperatures up to 65°C at Hg in methanol, b is not represented by the usual simple relation $b = RT/\beta\mathbf{F}$ but by Eq. [3].

The consequences of this situation with regard to the evaluation and significance of $\Delta H^{o\neq}_R$ are investi-